

Enhanced Heat Transfer Using Wire-Coil Inserts for High-Heat-Load Applications*

Jeff T. Collins, Craig M. Conley, John N. Attig

Advanced Photon Source, Argonne National Laboratory, Argonne, IL 60439, U.S.A.

Phone: (630) 252-6770, Fax: (630) 252-9350

e-mail: collins@aps.anl.gov

and

Michael M. Baehl

Summer Student Participant

Department of Mechanical Engineering, University of Illinois, Champaign, IL 61801, U.S.A.

Abstract

Enhanced heat-transfer techniques, used to significantly reduce temperatures and thermally induced stresses on beam-strike surfaces, are routinely used at the APS in all critical high-heat-load components. A new heat-transfer enhancement technique being evaluated at the APS involving the use of wire-coil inserts proves to be superior to previously employed techniques. Wire coils, similar in appearance to a common spring, are fabricated from solid wire to precise tolerances to mechanically fit inside standard 0.375-in-diameter cooling channels. In this study, a matrix of wire coils, fabricated with a series of different pitches from several different wire diameters, has been tested for heat-transfer performance and resulting pressure loss. This paper reviews the experimental data and the analytical calculations, compares the data with existing correlations, and interprets the results for APS front-end high-heat-load components.

Keywords: heat transfer, high heat load, wire coil, front end

1. Introduction

Shallow grazing-incidence-angles in conjunction with enhanced heat-transfer surfaces have been routinely used at the APS to significantly reduce temperatures and thermally induced stress on beam-strike surfaces. In the past, copper-mesh inserts, made from mesh rolled and compressed to a specific porosity, have been brazed inside of cooling channels of all front-end high-heat-load/flux components [1-3]. Although copper mesh provides extremely high-heat-transfer enhancement at low flow rates, relatively high pressure loss results consequently limiting the maximum usable cooling channel length. In addition, several maintenance issues arise associated with its use.

Several researchers have recently presented promising results using wire-coil inserts to enhance heat transfer within cooling channels [4-5]. This new heat-transfer-enhancement technique has since been extensively studied at the APS and will be used in place of copper mesh for all future APS high-heat-load/flux components. A large matrix of copper wire-coil inserts, fabricated from five different wire diameters over a wide

range of pitches, have been tested in a nonbrazed, mechanically inserted fashion for heat transfer and pressure-loss performance. All of the wire coils were tested in our standard 0.375-in-diameter test section, the same cooling channel size used in all APS front-end high-heat-load/flux components, using deionized water as the coolant. Several brazed wire-coil inserts have also been tested and compared with their nonbrazed counterparts. The wire-coil data matrix is expansive; including over a thousand individual data points and enough detail to allow optimization. This paper reviews the experimental data and the analytical calculations, compares the data with existing correlations, and interprets the results for APS front-end high-heat-load components.

2. Experimental Program

The test section schematically shown in Fig. 1, used for testing all of the nonbrazed wire-coil inserts, is made from oxygen-free high conductivity (OFHC) copper. The tube has a 0.50-in-OD, a 0.375-in-ID, and a length of 13.5-in. Two Kapton-encapsulated

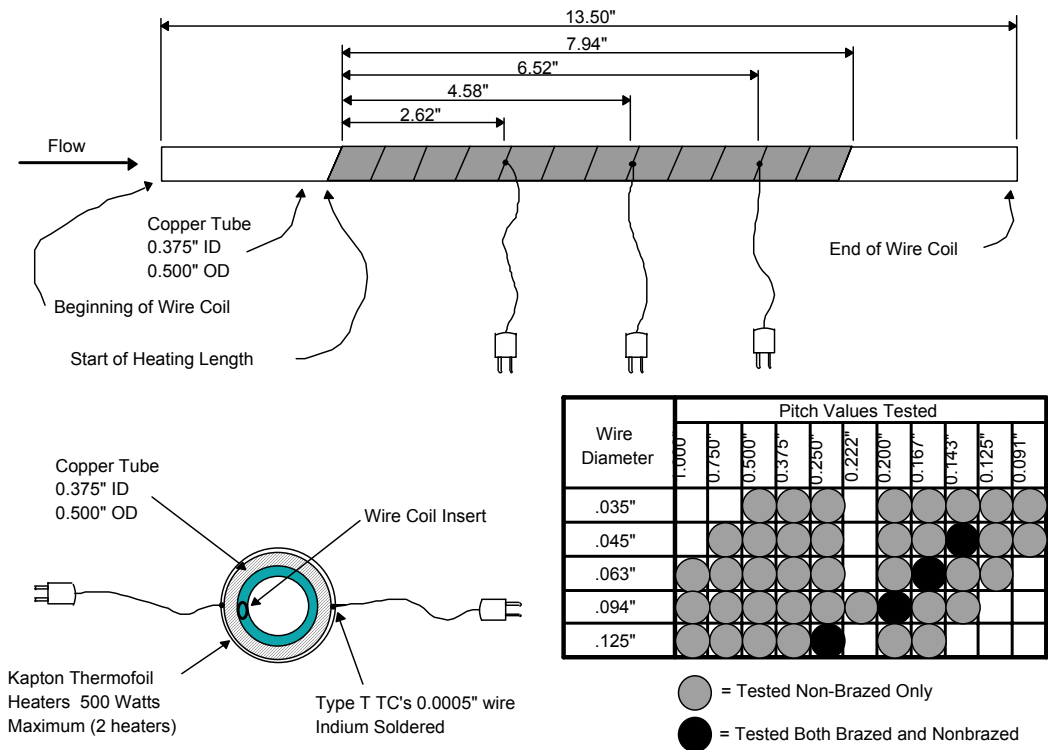


Figure 1: Schematic of the test section.

thermofoil heaters, rated at 250 W each, are continuously wrapped around the tube and bonded to the surface. At six locations between the heater wraps small shallow dimples are cut into the tube surface using a Dremel tool. Miniature copper-constantan thermocouples (TC) with 0.005-mil wire diameter are bonded to the tube surface, one at each shallow dimple, using an indium-eutectic solder. The soldering process is performed under a microscope to ensure that the thermocouple junction is located in the

center of the dimple, touching the bottom, with a minimal amount of solder to eliminate a potential surface-averaging effect. The six thermocouples represent three measurement nodes with two thermocouples at each node acting as an averaging group. The two thermocouples at each node are oriented 180 degrees apart and thus are located equal distances from the start of the heated length. The node positions are 2.62-in, 4.58-in, and 6.52-in from the start of the heating with a total heated length of 7.94-in. After fabrication, the entire tube was wrapped in silicon stretch tape to protect the heaters and thermocouples.

Also presented in Fig. 1 is a table detailing the wire-coil matrix for both the nonbrazed and brazed test samples. Five different wire sizes were chosen including 0.035-in, 0.045-in, 0.063-in, 0.094-in and 0.125-in. For each wire size, a range of pitch values were tested varying from 1-in down to 0.091-in depending on the wire size. Pitch refers to the distance between adjacent coils as measured from the centerline of the wire. All the wire coils tested were manufactured in-house by wrapping the wire around a precisely toleranced rod using the thread-cutting capabilities of a metal-working lathe. The diameter of the rod was chosen such that the final wire-coil OD provides a tight slip-fit when inserted into the test section. A variable tension wire-feed mechanism, designed and manufactured in-house, was added to the lathe to ensure uniform feed and tensioning during the wire-coil fabrication process. All the wire coils were fabricated to a 13.5-in length and extend from one end of the test section to the other when mechanically inserted.

All of the nonbrazed wire-coil inserts were tested in the same test section. The test section was attached to flexible flow lines via synthetic couplings to reduce axial heat loss and was placed in a trough and completely surrounded by vermiculite insulation to minimize radial heat loss. On the inlet flow-side of the trough, a coupling was added that could be disconnected to allow access to the inside of the test section. This provides easy insertion and removal of wire-coil inserts without disturbing the test section or the trough. A small nonintrusive hard stop on the downstream end of the test section ensured proper positioning of wire-coil inserts relative to the test section.

The four brazed wire-coil inserts, detailed in Fig. 1, were each vacuum brazed into a test section tube using eutectic silver/copper (72% Ag, 28% Cu) braze paste diluted with xylene. Two grams of braze paste were used per six inches of wire-coil length. The diluted braze paste is simply painted onto the wire coil prior to inserting into the test section tube, and then the tubes are vacuum brazed at around 800 degrees Celsius. The brazing process uniformly distributes the braze material onto all surfaces of the wire and the inside of the tube, integrally bonding the wire coil to the tube wall. After brazing, heaters and thermocouples were added to the tubes to create test sections identical to the one used for the nonbrazed wire-coil inserts.

The test section instrumentation includes instruments to measure mixed mean inlet and outlet temperatures and inlet-to-outlet differential pressure loss; a precision turbine flow meter for a majority of the flow range and a small orifice-type meter for flow rates below 1.0 gal/min (gpm); and the TC instrumentation. Uniform ohmic heat was applied

via a 2.0 kW capacity-regulated DC power supply. Power input was measured using a combination of a precision shunt for current measurements and precision resistors for the voltage measurements. The turbine flow meter and orifice-type meter were gravimetrically calibrated across their respective flow ranges to ensure very precise flow measurement. The flow range spans from 0.3 gpm to 5.0 gpm, with data collected in 0.1 gpm increments up to 1.0 gpm and in 0.25 gpm increments from 1.0 gpm to 5.0 gpm. The obtainable flow range for a given wire coil is limited by pressure loss at the high end and is limited by the heat transfer ability at the low end of the range resulting in an overheated test section. In general though, around 20 data points were collected for each wire coil.

All data were collected under steady-state conditions. The power was applied at a constant value of around 500 W, and the flow was incrementally changed across the flow range, allowing time to reach steady state at each increment. All of the data were collected using a customized data acquisition system, and the data were reduced using an in-house program. The inside wall temperatures needed to calculate the local heat transfer coefficient at the thermocouple locations were obtained in the conventional manner by subtracting the calculated copper-wall temperature drop from the measured outer wall temperatures under applied uniform heat flux.

3. Data Presentation

Figures 2 and 3 present the average heat transfer coefficient vs. water flow rate and pressure loss per inch of coil length vs. water flow rate, respectively, for wire-coil inserts

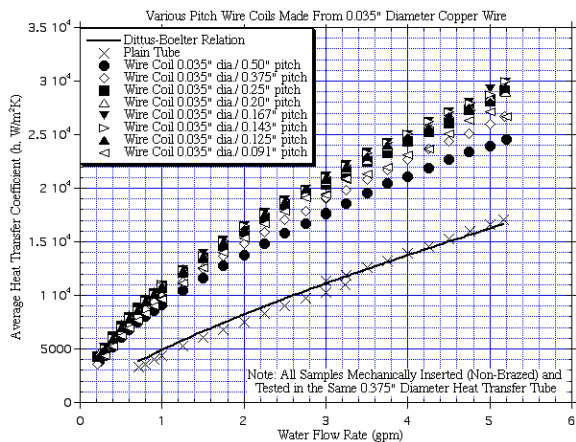


Figure 2: 0.035-in wire coils, h vs flow.

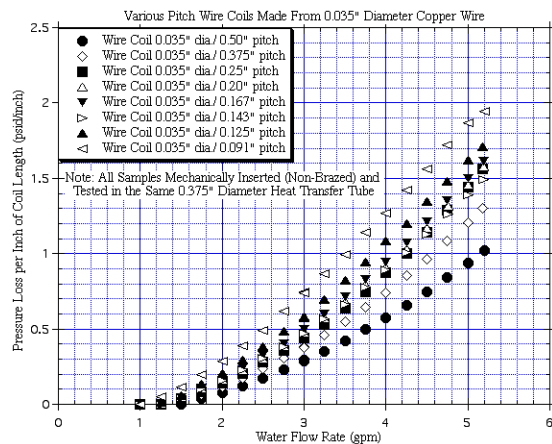


Figure 3: 0.035-in wire coils, ΔP vs flow.

made from 0.035-in-diameter wire. The average heat transfer coefficient (h) for all the data presented in this paper represents an average value from all three nodes. The calculated values at each node typically vary no more than five percent from one another, which is unprecedented in terms of the ability to measure heat transfer coefficients. The results for the test section with no wire coil installed, referred to as the “Plain Tube” in Fig. 2, varies no more than a few percent from the classic Dittus-Boelter relation, which predicts the heat transfer for plain smooth round tubes [6]. Excellent agreement with

Dittus-Boelter proves that the test section, data collection apparatus, and data reduction process are well founded and yield very accurate results. One can directly compare the Plain Tube to wire coils at a given flow rate and determine the level of heat transfer enhancement.

In the case of the 0.035-in wire-coil set, there is approximately two-fold enhancement, and, due to the narrow band of the data spread, it is obvious that the enhancement is not a strong function of pitch. An optimum exists in terms of maximum h at minimum flow rate at a pitch of between 0.143-in and 0.167-in. Corresponding to this point, a slight dip in pressure loss can be seen in Fig. 3 at a pitch of 0.143-in. Decreasing the pitch beyond this point causes an increase in pressure loss at a given flow rate.

Figures 4 and 5 present the average heat transfer coefficient vs. water flow rate and pressure loss vs. water flow rate, respectively, for wire-coil inserts made from 0.045-in-diameter wire. An optimum exists in terms of maximum h at minimum flow rate at a pitch of 0.167-in. On average, the level of heat transfer enhancement is slightly greater than two-fold, and the enhancement is a stronger function of coil pitch than for the 0.035-in wire-coil set as evidenced by a greater data span. In Fig. 5 note that a maximum occurs in terms of pressure loss vs. flow rate at a pitch of 0.167-in corresponding to the heat transfer results. Decreasing the pitch below this point actually causes less pressure loss at a given flow rate. This phenomenon shall be discussed in greater detail later in this paper.

For wire-coil inserts made from 0.063-in-diameter wire, Figures 6 and 7 present the average heat transfer coefficient vs. water flow rate and pressure loss vs. water flow rate, respectively. An optimum exists in terms of maximum h at minimum flow rate at a pitch of 0.20-in. The level of heat transfer enhancement is close to three-fold at this pitch, and the enhancement is a stronger function of pitch compared to the smaller diameter wire coils.

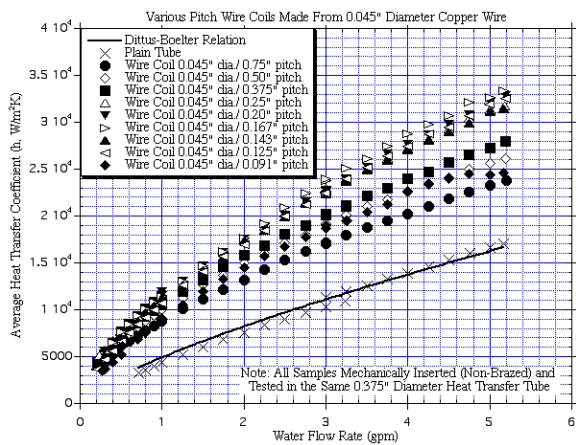


Figure 4: 0.045-in wire coils, h vs flow.

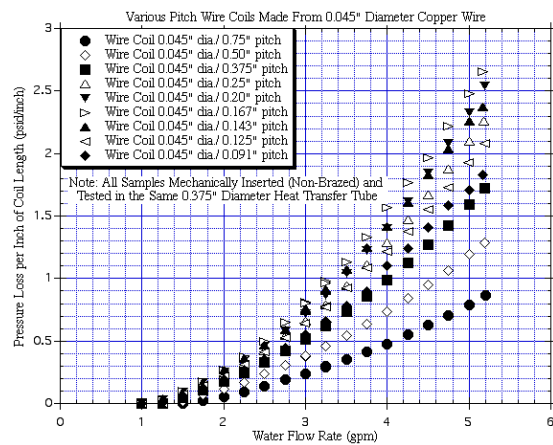


Figure 5: 0.045-in wire coils, ΔP vs flow.

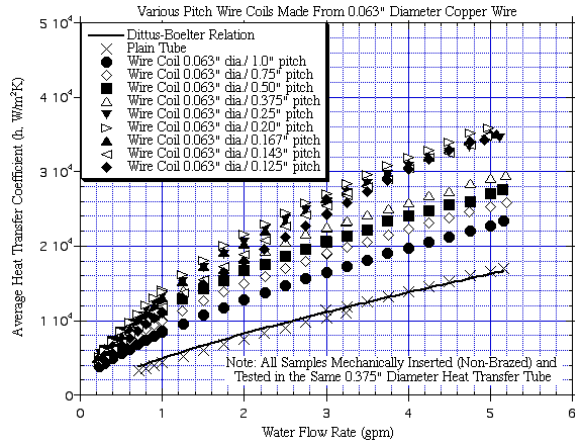


Figure 6: 0.063-in wire coils, h vs flow.

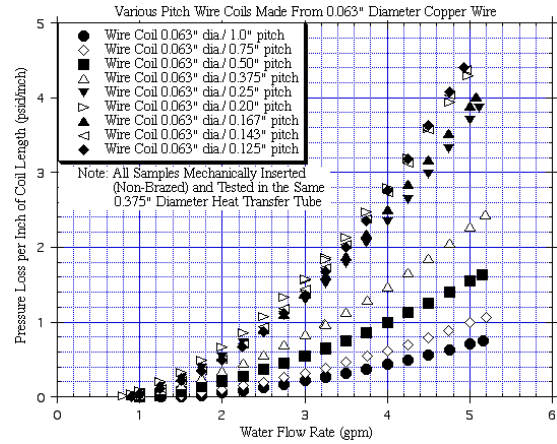


Figure 7: 0.063-in wire coils, ΔP vs flow.

Another interesting observation is that the 0.125-in-pitch wire coil, and to some degree the 0.143-in-pitch wire coil, have slightly steeper slopes in terms of h vs. flow rate compared to the larger pitch coils. In addition, the h vs. flow rate data seem to be concentrated in two distinct groups; one band of data for pitch values greater than or equal to 0.375-in and another band for pitch values less than or equal to 0.25-in pitch. A similar, though less distinct, trend can also be seen for the 0.045-in data. Similar to the 0.045-in wire-coil data, a maximum occurs in terms of pressure loss vs. flow rate at a pitch of 0.20-in corresponding to the heat transfer results. Decreasing pitch below this point causes less pressure loss at a given flow rate.

Figures 8 and 9 present the average heat transfer coefficient vs. water flow rate and the pressure loss vs. water flow rate, respectively, for wire-coil inserts made from 0.094-in-diameter wire. In terms of heat transfer, an optimum exists at a pitch of 0.222-in, representing an enhancement factor of approximately three-fold. Again, the heat transfer data seem to be concentrated in two distinct groups with the transition occurring at a pitch value of 0.375-in.

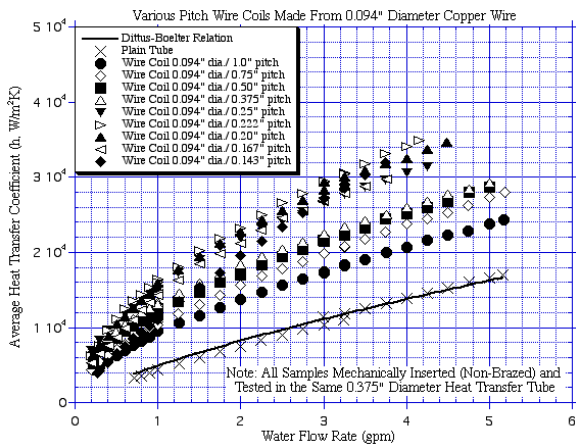


Figure 8: 0.094-in wire coils, h vs flow.

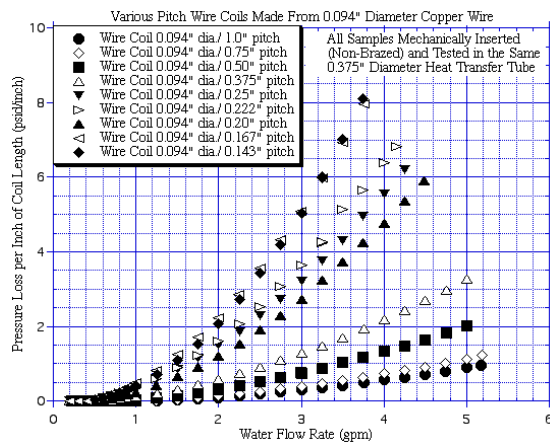


Figure 9: 0.094-in wire coils, ΔP vs flow.

This transition at a pitch of 0.375-in is also evident in the pressure loss vs. flow rate data, and, to a lesser degree, can also be seen with the 0.063-in wire-coil data. The data span is now a relatively strong function of wire-coil pitch. Also, the 0.143-in wire coil has a different, steeper slope compared to the other pitch wire coils in this data set. Similar to the 0.035-in wire-coil pressure loss data, a dip in pressure loss can be seen at a pitch value of 0.20-in. Decreasing the pitch beyond this point causes an increase in pressure loss at a given flow rate.

For wire-coil inserts made from 0.125-in-diameter wire, Figures 10 and 11 present the average heat transfer coefficient vs. water flow rate and pressure loss vs. water flow

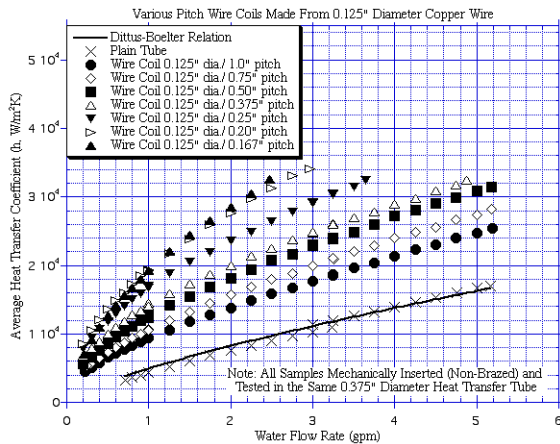


Figure 10: 0.125-in wire coils, h vs flow.

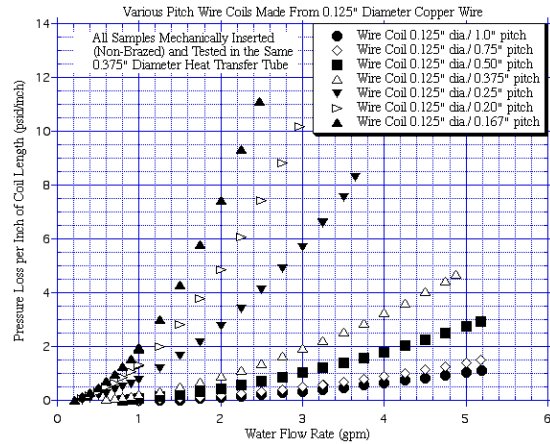


Figure 11: 0.125-in wire coils, ΔP vs flow.

rate, respectively. An optimum in terms of heat transfer no longer is evident, however, the curves for the 0.20-in- and 0.167-in-pitch wire coils are nearly identical indicating a near maximum. The data span is a strong function of wire-coil pitch, and an enhancement factor of nearly four-fold can be achieved with the tighter pitch coils. Although still existing to some degree, the trend for the data to appear in two distinct concentrated groups seems to be diminishing in terms of heat transfer. There is no longer any maxima or dips in the pressure loss data, but the transition point at 0.375-in still seems to exist. Pressure loss is also excessive compared with other wire diameters at a given flow rate.

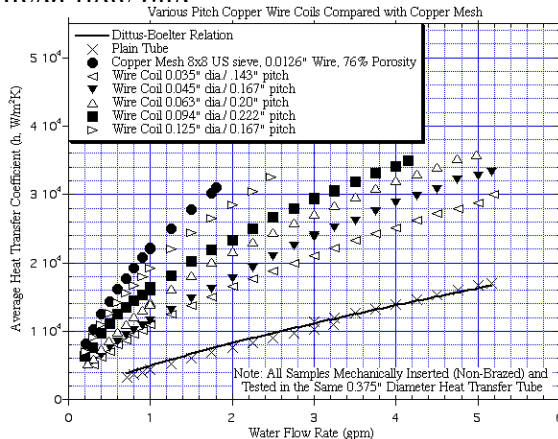


Figure 12: Mesh comparison, h vs flow.

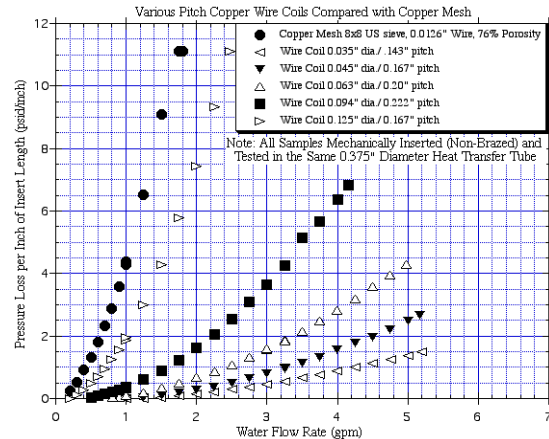


Figure 13: Mesh comparison, ΔP vs flow.

To summarize the data, Figures 12 and 13 compare the best wire-coil insert from each wire size to the APS standard porous mesh insert in terms of heat transfer vs. water flow rate and pressure loss vs. water flow rate, respectively. Although the mesh insert yields a higher heat transfer coefficient at a lower flow rate compared with the wire coils, the pressure loss is excessive. For example, the mesh insert yields $h=2 \text{ W/cm}^2\text{K}$ at a flow rate of 0.85 gpm compared with 1.05 gpm for the 0.125-in-diameter wire coil with a pitch of 0.167-in; however, the pressure loss for the mesh is nearly double that of the wire coil. Clearly, the mesh insert is much less efficient in terms of pressure loss that must be consumed to yield a desired heat transfer coefficient; this observation holds true across the entire flow range.

Figures 14 and 15 provide a comparison of selected brazed and nonbrazed wire coils in terms of heat transfer vs. flow rate and pressure loss vs. flow rate, respectively. For all

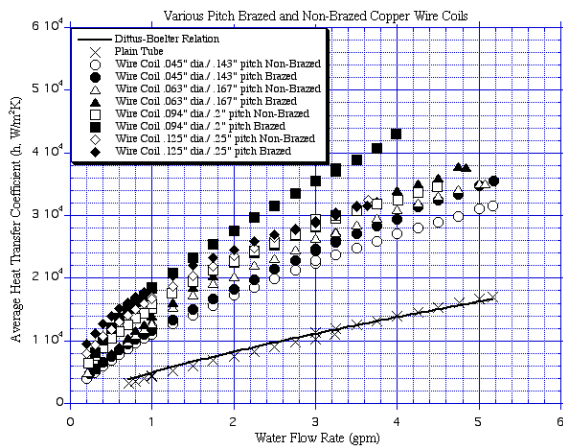


Figure 14: Brazed wire coils, h vs flow.

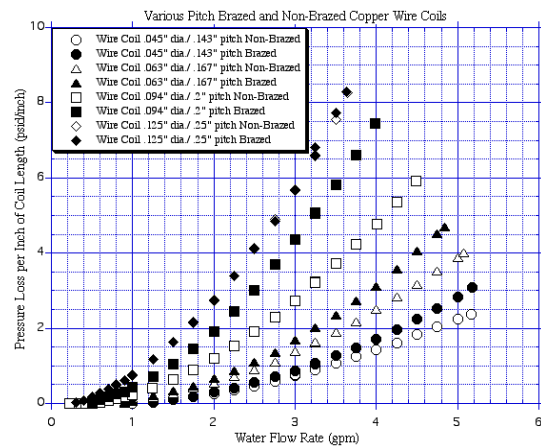


Figure 15: Brazed wire coils, ΔP vs flow.

of the wire coils except the 0.125-in-diameter wire, the brazing process increased both the heat transfer and pressure loss across the flow range. Also, with the exception of the 0.125-in-diameter wire coil, the degree of increase is amplified with increasing wire diameter; the greatest effect is seen with the 0.094-in-diameter wire coil. Only a slight increase in heat transfer occurs below 2.5 gpm for the brazed 0.125-in-diameter wire coil.

4. Data Analysis

Figures 2-11 provide a tremendous amount of information about nonbrazed wire coils in terms of data consistency, data span as a function of pitch and wire diameter, and identification of optimums, maximums, and transition points; however, viewing the data in a slightly different manner can reveal additional valuable information. Figures 16 and 17 represent a slice through all the nonbrazed wire-coil datasets at $h=1.5 \text{ W/cm}^2\text{K}$ presenting water flow vs. pitch and pressure loss vs. pitch, respectively. Similar plots are also presented at $h=2.0 \text{ W/cm}^2\text{K}$ and $h=2.5 \text{ W/cm}^2\text{K}$ in Figures 18 and 19 and Figures 20 and 21, respectively. The flow rate vs. pitch plot clearly show an optimum value for each wire diameter occurring at a minimum flow-rate point. This point occurs more gradually with the smaller diameter wires and progressively becomes sharper with increased wire

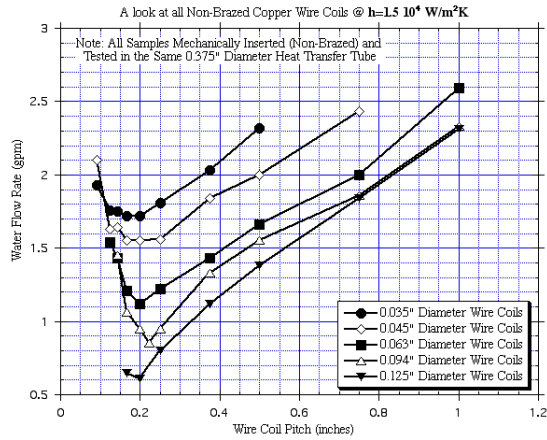


Figure 16: Slice @ $h=1.5$, flow vs pitch.

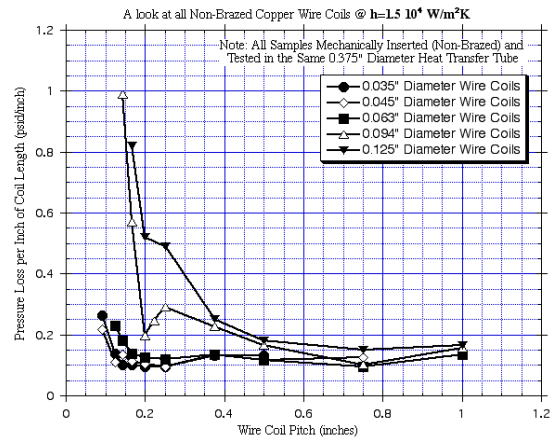


Figure 17: Slice @ $h=1.5$, ΔP vs pitch.

diameter. Decreasing the pitch below the minimum flow-rate point causes a rapid rise in both water flow rate and pressure loss required to sustain a desired heat transfer coefficient. Although curve shapes appear similar for each of the flow rate vs. pitch plots, the y-axis scales are different for each. The amplitude of the flow rate vs. pitch curves for each wire diameter therefore increases significantly with increasing heat transfer coefficient. Another interesting observation for the flow rate vs. pitch plots is that, except for the 0.035-in-diameter wire-coil set, an upward hump in the data exists between a pitch range of approximately 0.25-in to 0.75-in with an inflection point on the hump occurring at approximately 0.375-in, the test-section diameter.

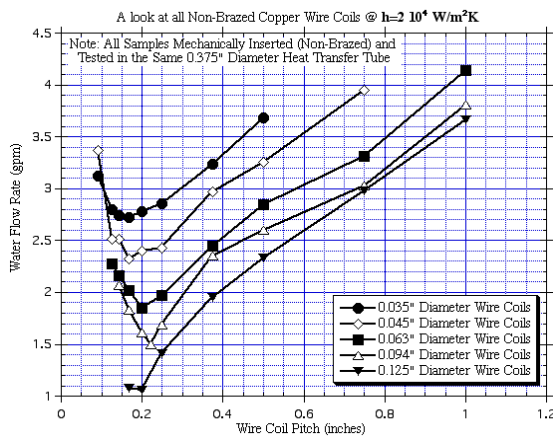


Figure 18: Slice @ $h=2.0$, flow vs pitch.

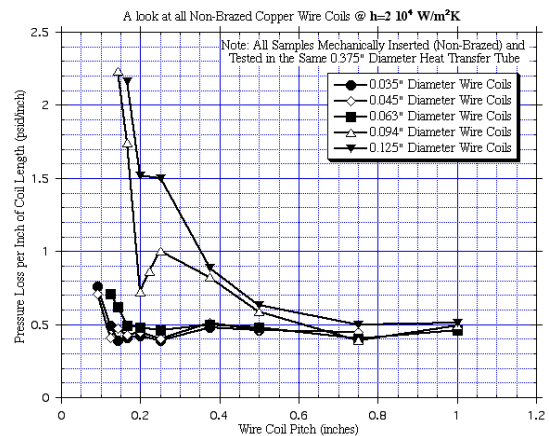


Figure 19: Slice @ $h=2.0$, ΔP vs pitch.

This same hump behavior can be observed over the same 0.25-in to 0.75-in pitch range in the pressure loss vs. pitch plots. It seems that the 0.035-in- to 0.063-in-diameter wire coils have an inflection point at 0.375-in, corresponding to the flow rate vs. pitch plots, whereas the 0.094-in- and 0.125-in-diameter wire coils have their inflection points at around 0.25-in. For wire diameters 0.063-in and smaller, the pressure loss vs. pitch curves appear nearly identical, almost lying on top of one another. Both the 0.094-in-

and 0.125-in-diameter wire coils exhibit a transition or dip between 0.25-in and 0.20-in pitch. For these coils, decreasing the pitch below 0.20-in causes a rapid rise in pressure loss to sustain the same heat transfer coefficient.

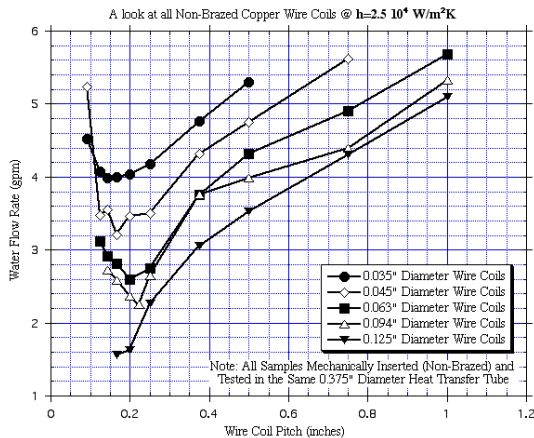


Figure 20: Slice @ $h=2.5$, flow vs pitch.

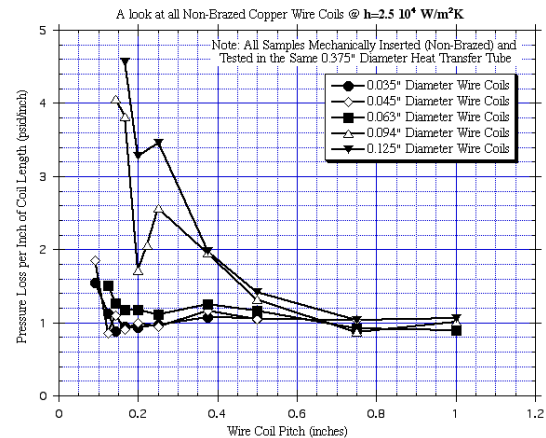


Figure 21: Slice @ $h=2.5$, ΔP vs pitch.

The authors theorize that three distinct flow regimes exist that govern the wire coil performance. In general, spiral-dominant flow exists for pitch values greater than around 0.25-in. In this regime, flow through the channel has a large spiral component; the entire flow field has an auger-like motion. As pitch is decreased below this point, a transition zone is encountered where the fluid boundary layers against the tube wall are minimized. As the pitch is decreased further, a new flow regime is entered which is core-flow dominant. In this regime, the pitch has become so tight that the water begins to slip over the wires and the spiral-flow pattern rapidly diminishes. Some spiral flow probably still occurs, but a majority of the flow passes through the center of the wire coil and flow at the tube wall diminishes.

5. Conclusions

The use of wire-coil inserts to significantly increase heat transfer at reasonably low flow rates offers great benefit to the synchrotron community. High levels of heat transfer can be achieved with substantially less resulting pressure loss compared to previously employed heat-transfer-enhancement techniques. When compared to copper-mesh inserts this reduction in pressure loss is evident. Additionally, unlike mesh inserts, wire-coil inserts impose far fewer concerns in terms of water quality, clogging, or erosion. This is especially true for wire coils made from large wire diameters in terms of erosion/corrosion concerns. For the APS, we have chosen to use the 0.094-in-diameter wire coil with a pitch of 0.20-in for the new canted-undulator front-end design [7]. For the design heat transfer coefficient of $2.0 \text{ W/cm}^2\text{K}$, the chosen wire coil will require a flow rate of 1.6 gpm if nonbrazed, or a flow rate of 1.1 gpm if brazed. The corresponding pressure loss per inch of coil length will be around 0.75 psid/inch if nonbrazed or 0.60 psid/inch if brazed due to the lower flow requirement. Brazing the wire coils is therefore desirable since less flow will be required and consequently less pressure loss will occur.

6. Acknowledgments

The authors thank Dr. Tetsuro Mochizuki from SPring-8 for providing the APS information on wire-coil heat-transfer-enhancement technology. The authors also thank S. Picologlou for editing this paper. This work was supported by the U.S. Department of Energy, Office of Basic Energy Sciences, under Contract No. W-31-109-ENG-38.

7. References

- [1] T. Kuzay and J. Collins, "Heat Transfer Augmentation in Channels with Porous Copper Inserts," NATO ASI paper, ASI97/0275600m-m, 1999
- [2] T. Kuzay, J. Collins, A. Khounsary and G. Morales, "Enhanced Heat Transfer with Wool-Filled Tubes," ASME/JSME 3rd Joint Heat Conference, Book No. I0309E-1991, Reno, Nevada, pp. 145-151
- [3] T. Kuzay, J. Collins and J. Koons, "Boiling Heat Transfer in Channels with Porous Copper Inserts," International Journal of Heat and Mass Transfer, 1999, pp. 1189-1204
- [4] S. Sharma, C. Doose, E. Rotela and A. Barcikowski, "An Evaluation of Enhanced Cooling Techniques for High-Heat-Load Absorbers*," MEDSI02 publication, 2002
- [5] T. Takiya, T. Mochizuki, H. Kitamura, "Development of Enhanced Heat Transfer Coolant Channels for the SPring-8 Front End Components," SPring-8 document, 2001
- [6] J. Holman, *Heat Transfer*, McGraw-Hill Book Company, p. 274-276, 1986
- [7] Y. Jaski, E. Trakhtenberg, J. Collins, C. Benson, B. Brajuskovic and P. Den Hartog, "Thermomechanical Analysis of High-Heat-Load Components for the Canted-Undulator Front End," MEDSI02 publication, 2002